npj | flexible electronics

Article

Published in partnership with Nanjing Tech University

https://doi.org/10.1038/s41528-025-00387-7

Locomotion control of Cyborg insects by using ultra-thin, self-adhesive electrode film on abdominal surface

Shumpei Katayama[1,2], Keigo Ando[1,2], Sunghoon Lee[1,3], Zhi Jiang[4], Xiaodong Chen[4], Tomoyuki Yokota[5,6], Hirotaka Sato[7], Shinjiro Umezu[2] ✉, Kenjiro Fukuda[1,3] ✉ & Takao Someya[1,3,5] ✉

Cyborg insects are living organisms combined with artificial systems, allowing flexible behavioral control while preserving biological functions. Conventional control methods often electrically stimulate sensory organs like antennae and cerci but these invasive methods can impair vital functions. This study shows a minimally invasive approach using flexible, ultra-thin electrodes on the cockroach's abdomen, avoiding contact with primary sensory organs. Using liquid evaporation for film adhesion provides a biocompatible process with excellent adhesive strength and electrical durability. Body surface stimulating component structures formed by utilizing an insect's natural movement showed higher stability than conventional methods. These enable effective control of both turning and straight-line movements. This minimally invasive method maintains the insect's natural behavior while enhancing cyborg functionality, extending the potential applications.

Cyborg insects, which represent a fusion of living organisms with artificial systems are capable of flexible adaptation and free behavioral control[1]. With advancements in robotics research, body flexibility and locomotion have become increasingly important[2–4]. Efforts are progressing that focus on the flexibility of living animals and the technologies for controlling animal behavior through external stimuli while preserving the organism's biological functions[5–9]. Cyborg insect systems are advancing towards functional robotic applications[10–15], and barriers related to autonomous control mechanisms and power supply are being overcome[16–18]. This holds promise for practical applications in areas such as disaster rescue[13], mapping[19], and environmental monitoring[20]. To continue improving the abilities of cyborg insects, minimally invasive device integration must be developed that does not interfere with the insect's physiological functions[16,21].

Cockroaches are frequently used as models for studying insect leg locomotion and escape behaviors, and their mobility has been well studies[22–24]. Among them, *Gromphadorhina portentosa* (*G. portentosa*, the Madagascar hissing cockroach), one of the largest species, is particularly suitable for the development of cyborg insect technology due to its ability to pull several times its body weight[25] and its relatively slow walking speed compared to other cockroach species[26].

Conventional motion control in cockroaches induces natural responses[27–29] by stimulating their antennae[30,31], cerci[32,33], or ganglia[34]. Although insects respond to vibrations[35], heat[36], and chemicals[37], control through electrical stimulation by a direct current applied to the biological tissues remains the most common due to its controllability and low power consumption. Stable electrophysiological contact between the biological tissue and the electrode is crucial for effective electrical stimulation[38]. Typically, the insertion and fixation of microwire electrodes into the target tissue is the standard approach. This raises lead to concerns regarding electrode degradation due to tissue contact[39,40] and the electrode position drifting because of movement[41,42]. To address these issues, research has been conducted on developing stable microwire electrodes for use in vivo[43], establishing electrically stable structures by inserting electrodes pre-adulthood[44], and forming conductive hydrogel electrodes on the surface of the antenna[21].

However, developing minimally invasive behavioral control techniques that do not affect the insect's primary sensory organs remains challenging. The currently reported target body parts for stimulation are limited to the antennae, cerci, and ganglia. Since the antennae are crucial for object detection and decision-making during movement[45–47], while the cerci are

[1]RIKEN Center for Emergent Matter Science (CEMS), Wako, Saitama, Japan. [2]Department of Modern Mechanical Engineering, Waseda University, Shinjuku-ku, Tokyo, Japan. [3]Thin-Film Device Laboratory, RIKEN, Wako, Saitama, Japan. [4]Innovative Center for Flexible Devices (iFLEX), Max Planck-NTU Joint Lab for Artificial Senses, School of Materials Science and Engineering, Nanyang Technological University, Singapore, Singapore. [5]Department of Electrical Engineering and Information Systems, Graduate School of Engineering, The University of Tokyo, Tokyo, Japan. [6]Institute of Engineering Innovation, Graduate School of Engineering, The University of Tokyo, Bunkyo-ku, Tokyo, Japan. [7]School of Mechanical and Aerospace Engineering, Nanyang Technological University, Singapore, Singapore. ✉e-mail: umeshin@waseda.jp; kenjiro.fukuda@riken.jp; takao.someya@riken.jp

important for detecting approaching objects and functioning as equilibrium organs[29,48], invasive insertion or the attachment of stimulation electrodes to these sensory nerves could potentially impair the insect's essential abilities.

In this paper, we present a method for behavioral control through electrical stimulation applied externally to the abdominal surface. This method neither contacts their primary sensory organs nor causes any damage during implementation. Flexible ultra-thin film electrodes were attached to the insect's abdomen using a bio-compatible adhesion method with assist of polar solvent such as water and ethanol. This method exerts approximately 160 times greater more adhesion energy along with enhanced electrical durability compared to commercial electrode paste. The newly developed adhesive layer affords the more stable application of thinner films onto the insect's exoskeleton. By electrically stimulating the lateral abdominal surface through these integrated electrodes, we achieved control of turning movements and straight-line acceleration. This non-invasive control method, unconnected to the insect's primary sensory organs, allows for the natural utilization of the insect's exceptional behavioral characteristics.

Results

Components and structures of electrical stimulation on insect abdominal surface

Gromphadorhina portentosa (*G. portentosa*, Madagascar hissing cockroach) specimens were used as the subjects to implement the proposed method. The body surface stimulation components were attached to the dorsal abdomen (Fig. 1a). These components comprised three different functional films: an interfacial film for adhesion between the body surface and upper film, a wiring film, a self-adhesive body surface stimulation film (Fig. 1b). Styrene-ethylene-butylene-styrene (SEBS) thermoplastic elastomer was used as the interfacial adhesion film. This material is known for its high self-adhesiveness and stretchability[49]. It adhered closely to the insect's body surface, forming a stable adhesive interface. A film of Cr (3.5 nm) and Au (100 nm) deposited on a 2 μm thick parylene substrate was used as the wiring film. The Au/SEBS (50 nm/1 μm) film was used as the self-adhesive body surface stimulation film. It has metal particles that partially protrude from the polymer surface, forming a self-adhesive conductive interface[49]. As discussed later, to optimize the experiment, the thicknesses of the interfacial, wiring, and self-adhesive body surface stimulation films were set to 1 μm, 2 μm, and 1 μm with the total thickness being approximately 4 μm where all films overlapped (Fig. 1c). The stimulation film conformably adhered around the tail for electrical stimulation (Fig. 1d). The wiring film mostly adhered with interfacial film but partially free-standing to be bent outward at the overlapping segments (Fig. 1e).

Most of the insect's body is covered by a smooth, curved exoskeleton, is waterproof, abrasion resistant[50] and movable thus ensuring flexibility[51,52]. These features make affixing the device to the exoskeleton's chitinous surface challenging. The stimulation film is self-adhesive, but simply pressing it onto the insect's uneven and micro-patterned body surface does not ensure uniform adhesion. By using a wet-volatile process, introducing ethanol between the insect and the film during application and allowing it to

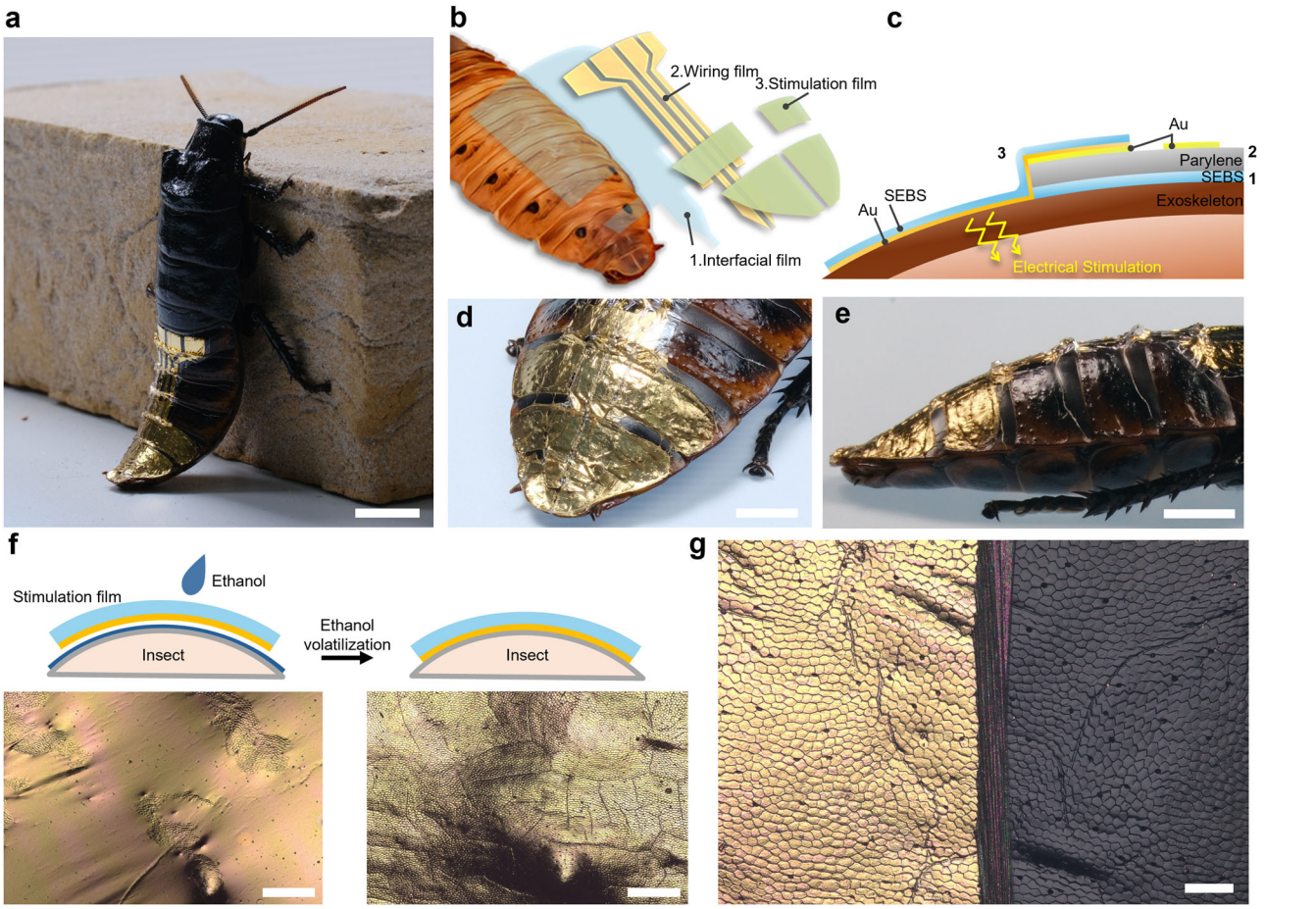

Fig. 1 | Components and structures of electrical stimulation on insect abdomen. **a** *G. portentosa* with the integrated body surface stimulation component on the abdominal surface. Scale bar, 1 cm. **b** Schematic of body surface stimulation component. **c** Layered structure of body surface stimulation component. **d** Closs-up view photo of integrated body surface stimulation component on the abdominal surface. Scale bar, 5 mm. **e** Side view photo of integrated body surface stimulation component on the abdominal surface. Scale bar, 5 mm. **f** Integration process of self-adhesive body surface stimulation film on the insect's body surface. Before ethanol volatilization (left), after ethanol volatilization (right). Scale bar, 200 μm. **g** Self-adhesive body surface stimulation film adhered to insect body surface (left), natural insect body surface (right). Scale bar, 50 μm.

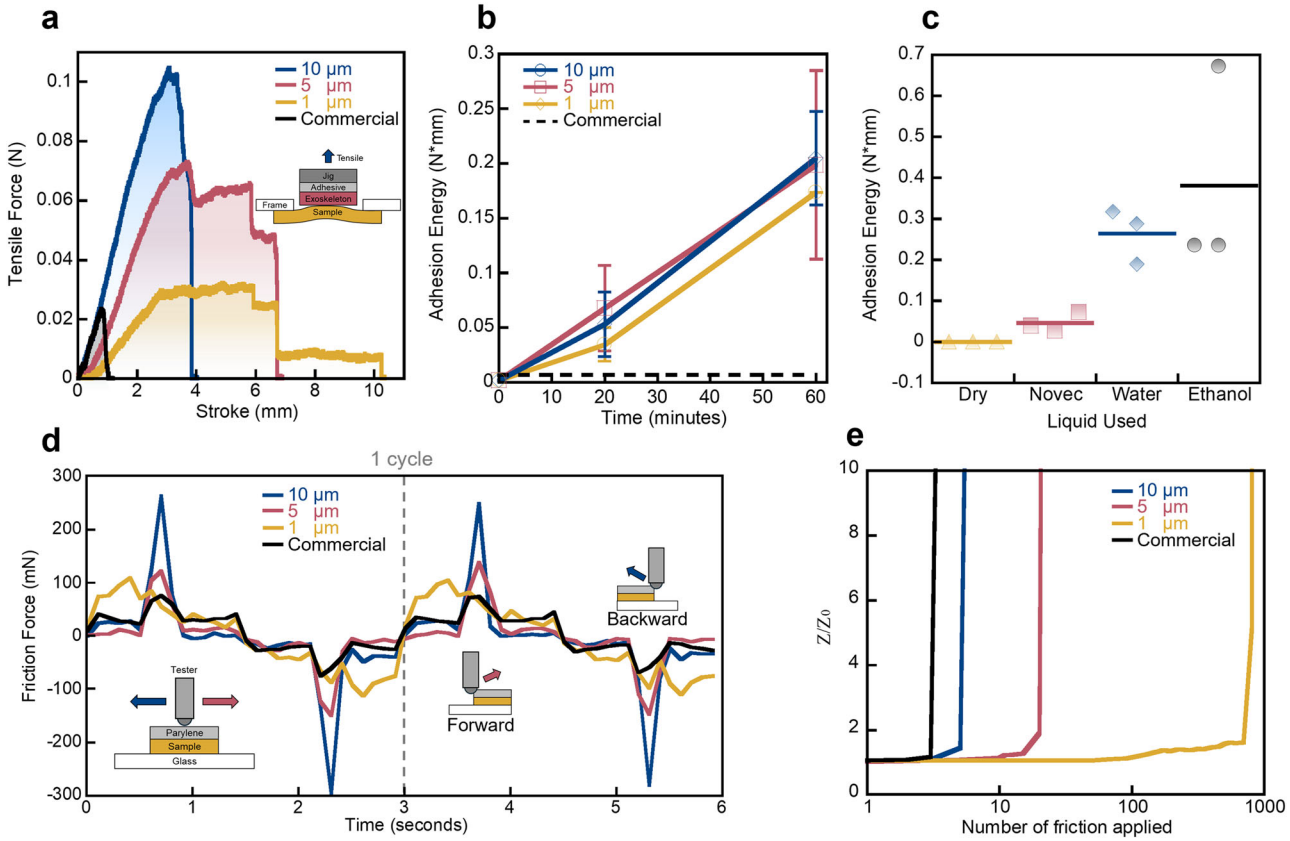

Fig. 2 | Adhesion of self-adhesive body surface stimulation film. a Tensile stroke-force characteristics of the 10, 5, and 1 μm thick self-adhesive body surface stimulation film adhered to insect exoskeleton by wet-volatile process using ethanol. And commercial electrode paste adhered with insect exoskeleton. Tests were conducted three times in each condition. For each condition, the data of the maximum adhesion energy is shown in the graph. **b** Ethanol volatilization time - adhesion energy (the integral of the stroke and tensile force) characteristics of adhesion conditions same as in (**a**). **c** Tensile stroke-force characteristics depending on the liquid used for wet-volatile process when 10 μm thick self-adhesive body surface stimulation film adhered to the insect exoskeleton. Tests were conducted three times in each condition. Lines indicate average values. **d** Friction force characteristics of the 10 / 5 / 1 μm thick self-adhesive body surface stimulation film and commercial electrode paste adhered to glass. Forward and backward indicate when the instrument contacted the film from each direction, and the maximum force was measured. In each condition, the test was performed once. **e** Number of friction applied—impedance change characteristics when same conditions as in (**d**).

evaporate completely, the film adheres conformally to the surface (Fig. 1f). The film conforms well to the shape of the insect's abdomen, allowing its surface shape to be clearly observed from above (Fig. 1g).

Adhesion of self-adhesive body surface stimulation film

The self-adhesive body surface stimulation film's bonding properties for attachment to the insect's body surface were evaluated as were the requirements for the wet-volatile process. A specimen exoskeleton was cut into 5 mm squares and attached to an upper jig, and the film bearing the lower jig was affixed to it. The adhesive strength was evaluated by measuring elongation and force during a vertical tensile test (Supplementary Fig. 1). Using ethanol as the liquid to assist adhesion, a film with 50 nm of Au deposited on 10 μm and 1 μm thick SEBS was bonded to the body surface. The volatilization time for this process was one hour. The maximum forces recorded were approximately 1.04×10^{-1} N and 3.2×10^{-2} N, with elongations of approximately 4.0 mm and 10.2 mm. In contrast, when a commercial electrode paste (Elefix Z-181BE, NIHON KOHDEN) was used, the maximum force was approximately 2.3×10^{-2} N. The elongation in this case was approximately 1.2 mm (Fig. 2a).

To establish any connection between the ethanol vaporization time and bonding force, the duration was varied from 0 to 60 min. The vertical adhesion strength was then calculated as the adhesion energy, which is defined as the integral of the stroke and tensile force[53]. Regardless of the SEBS thickness, the adhesion energy showed a tendency to increase with longer volatilization times. At 60 min, when ethanol was considered fully evaporated, no significant difference in adhesion energy was observed between different SEBS thicknesses. The adhesion energy was approximately 26 to 31 times higher (Fig. 2b) than that of the commercial electrode paste, which exhibited no change in adhesion strength over time.

Experiments were also conducted by changing the fluid material used for adhesion to evaluate how the fluid material affect the adhesion. Under fluid-free conditions, the maximum force was 1.3×10^{-3} N. Comparatively, Ethanol exhibited an approximately 160 times higher adhesive force at 2.0×10^{-1} N. Deionized water and Novec7100 (fluorinated solvent) respectively produced 1.3×10^{-1} N, 4.1×10^{-2} N. While water and ethanol demonstrated similar adhesive strengths, Novec7100's adhesive force was an order of magnitude lower (Fig. 2c). The reason that ethanol exhibited the highest adhesive strength may be due to the following mechanism. Anhydrous ethanol temporarily dehydrates the SEBS, causing it to lose self-adhesiveness. After losing adhesiveness, ethanol penetrates the interface between the SEBS and the body surface, but as the ethanol volatilizes the SEBS approaches the body surface. Once sufficiently close, the SEBS should uniformly adhere to the insect's surface by van der Waals forces. It was also confirmed that the ethanol permeability of Au/SEBS increases as its with thickness decreases (Supplementary Fig. 2). If the film is sufficiently thin, ethanol is likely to permeate it and evaporate effectively. Conversely, adhesion did not improve in by changing the wet-volatile process drying time for the 500 nm thick parylene/Au film, which has no self-adhesive properties and has very low ethanol permeability (Supplementary Fig. 3). Therefore, using an ethanol wet-volatile process for attaching the self-

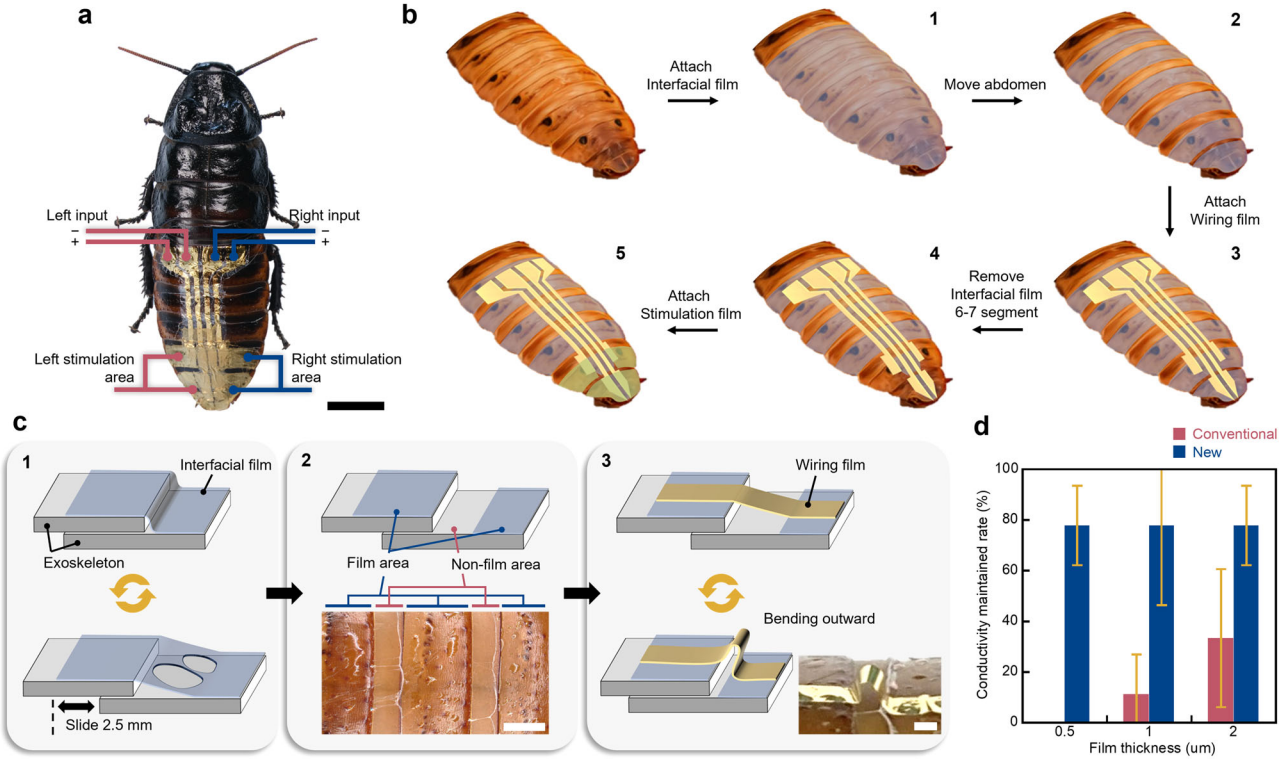

Fig. 3 | Integration of body surface stimulation component. a The body surface stimulation component seen from the top. The contact area between the insect body surface and the self-adhesive body surface stimulation film is shown as the stimulation area, the external input position of electrical stimulation. **b** The process of integrating the body surface stimulation component onto the insect body surface. Some details of the 1–3 process are shown in **c**. **c** Schematic image of interfacial film produced by abdominal movement. The top-mounted wiring film takes an outward bend. Panels 1–3 supports (**b**), 1–3. Photograph of image 2, scale bar, 2 mm. Photograph of image 3, scale bar, 1 mm. **d** Characteristics of conventional integration methods and this method. Showing the rate of impedance keeping below 1 kΩ for 0.5, 1.0, and 2.0 μm-thick wiring films. In each condition, tests were performed three times in three individuals each. The yellow lines represent the standard deviation for each condition.

adhesive body surface stimulation film, was confirmed to provide superior adhesion strength compared to the commercial electrode paste.

The self-adhesive body surface stimulation film's durability against friction was also assessed. For cyborg insects demanding activity in confined environments, durability against friction is an important parameter. The self-adhesive body surface stimulation film was attached to a substrate and subjected to a load from above. Friction was applied and its directional force was measured. The friction force was as its maximum when overcoming the film and strong force is involved in the film (Fig. 2d). The maximum forces recorded under conditions with SEBS thicknesses of 1, 5, and 10 μm were 110, 150, and 290 mN. This indicates that thicker SEBS layers generate greater forces under friction. The impedance of the film was measured against the number of friction cycles. For the commercial electrode paste, the impedance increased significantly, reaching 48.8 times the initial value after five friction cycles. In contrast, with a SEBS thickness of 1 μm, the impedance increased only 1.1 times after five friction cycles and 1.6 times after 700 cycles. Complete failure occurred at around 800 cycles, with the impedance increasing approximately 1.4 million times. This demonstrates that the self-adhesive body surface stimulation film is highly durable against friction. However, with SEBS thicknesses of 5 μm and 10 μm, a sudden increase in impedance due to rupture was observed after 25 and 10 cycles (Fig. 2e). Electrodes with thinner SEBS layers are likely to experience lower loads during friction compared to those with thicker layers, resulting in higher electrical durability. Additionally, films with a thicker SEBS layer were observed to peel off at the edges, while those with a thinner SEBS layer wore away at the edges (Supplementary Fig. 4). This suggests that if the film's fracture strength is higher than the frictional force applied, it tends to detach more easily due to friction. Since further reduction of thickness caused handling problems, we concluded 1 μm SEBS layer was optimal.

Integration of body surface stimulation components

A method was established to integrate body surface stimulation components suitable for the abdominal movements of insects. The structure only makes electrical contact with the surface of and sixth and seventh/eighth abdominal segments. The contact areas on the left and right sides of the insect's body are electrically stimulated between the contact area of the sixth segment and those of the seventh-eighth segments. The left side controls movement to the left, and the right side controls movement to the right (Fig. 3a).

The body surface stimulation components are integrated through five steps (Fig. 3b). First, the interfacial film was adhered to the insect's cleaned abdominal surface using ethanol for the wet-volatile process (Fig. 3b-1). Then, abdominal contraction and extension movements were induced. During deformation, the segments were seen to overlap. This damaged the interfacial film due to mechanical over-stretching beyond its (Fig. 3c-1) with the interfacial film only remaining in the non-overlapping areas. This formed an alternating adhesive-non-adhesive interleaving structure (Fig. 3b-2, c-2). After forming this structure, the wiring film was bonded to the dorsum of the fully stretched abdomen with its Au side facing upwards. When the insect's abdomen contracted, the wiring film bent outward. This preserved the insect's mobility while maintaining a stable wiring structure for conduction (Fig. 3b-3, c-3).

Next, the interfacial film on the sixth and seventh-eighth abdominal segments was wiped off with ethanol (Fig. 3b-4). The self-adhesive body surface stimulation film was then adhered using the wet-volatile process, ensuring that the Au side contacted the insect's body surface. This established conductivity with the wiring film. By again inducing abdominal movement, the self-adhesive body surface stimulation film between the sixth and seventh/eighth abdominal segments is torn. The connection between the seventh and eighth segments is secured by the wiring film

spanning the segments. Finally, portions of the self-adhesive body surface stimulation film are removed to isolate the conductive structure (Fig. 3b-5). The initially adhered interfacial film acted as an adhesive layer for the wiring film and an insulating layer between the self-adhesive body surface stimulation film and the insect. This process formed a 1–4 μm thick body surface stimulation component that adapted to the insect's abdominal movement.

The impact of this SEBS interfacial layer on the stability of the wiring film's conductivity was evaluated by comparing it with the conventional method (using commercial resin based liquid adhesive) of attaching film electronics to the abdominal surface[16]. The wiring films with variously thick parylene layers were applied to the insect's abdomens using both new and conventional methods. The rates at which conductivity (impedance) remained below 1 kΩ after abdominal movement were assessed. In the conventional methods, conductivity retention decreased as the parylene layer thickness in the wiring films was reduced. At a thickness of 2 μm, approximately 33% of the wiring films retained conductivity, but this dropped to 0% at 0.5 μm. In contrast, the SEBS interfacial layer maintained a high rate of conductivity regardless of film thickness. Even at a film thickness of 0.5 μm, conductivity retention was approximately 78% (Fig. 3d). This is probably because, the SEBS interfacial layer forms the wiring film's adhesive surface before attaching it. Conversely, the conventional methods require abdominal stretching as the liquid adhesive solidifies. This process causes excessive stress on the wiring film. The SEBS interfacial layer enables more delicate wiring film to be integrated without damage.

Verification of the body surface stimulation components' efficacy

The components adhered to the insect's body surface afford control of the insect's left and right directional movements. It has been reported that when *G. portentosa* is stimulated by stroking the surface of its abdomen along the side, the abdomen yaws toward the stimulated side while the legs on that side inflect inward and the leg on the opposite side inflect outward[35]. This reaction is strong when stimulating rear segments (Supplementary Movie 1). Inducing this response and forward movement through electrical stimulation generates a turning motion toward the stimulated side. This same stimulation is electrically applied by film electrodes on the surface of the abdomen to control leftward and rightward movements. When the left side of the abdomen is stimulated, the abdomen yaws to the left, causing inward flexion of the left leg and outward extension of the right leg. This produces in forward movement and a leftward turn (Fig. 4a).

To confirm that proper stimulation was applied, the impedance between the stimulation components and the insect's body was measured. Lower impedance between the electrodes and the insect is advantageous for electrical stimulation[21]. At the control frequency of 40–50 Hz, the impedance was 4.5×10^4 Ω for the conventional method that fixes a microwire inside the body, and 5.1×10^4 Ω for the proposed stimulation method (Fig. 4b). Typically, the method of fixing electrodes inside the body evidences lower impedance, but the proposed method maintains similar impedance. This is probably due to greater contact between the electrodes and the insect. In the conventional method, the contact area is approximately 5.0×10^{-2} mm^2 with the wire electrode (0.08 mm diameter, 10 mm insertion). In contrast, the surface stimulation method's, contact area is approximately 15 mm^2 (individual differences exist). This larger contact area probably contributes to the sufficiently low impedance. In the conventional method, the impedance between the insect and the electrode tended to increase with time after the electrode was placed[40]. However, this method showed no increasing trend even after 72 h. (Supplementary Fig. 5). Therefore, it is indicated this method can be used stably for a longer time than the conventional method.

To verify the insect's responsiveness to the electrical stimulation components, movements were induced by a 2-second stimulus at voltages ranging from 1 to 8 V. At voltages of 2 V or below, the induced turning motion in both directions averaged less than 20 degrees, indicating no significant turning motion. However, at 6 V, significant turning responsiveness was observed, with approximately 70 degrees of turning in each direction. As the applied voltage increased, a larger turning angle was observed (Supplementary Movie 2). Conversely, the difference between the maximum and minimum turning angles increased as the voltage increased, making the control differences between individuals more pronounced (Fig. 4c, d). Therefore, the voltage must be adjusted based on individual differences. When setting the voltage without considering individual differences, 6 V is suggested as appropriate. At this voltage, significant left and right directional control was observed, and the standard deviation in each direction was within an acceptable range. The positional change before and after the 6 V electrical stimulation is shown in Fig. 4e, demonstrating that leftward and rightward turning can be effected through body surface electrical stimulation, as with conventional methods.

Furthermore, by stimulating control areas on both the left and right sides at the same time, the insect can be directed to accelerate straight forward. This enables obstacles to be overcome more efficiently compared to the absence of stimulation. When stimulated, it took only 1.5 s to traverse the obstacle, but when not stimulated, it took more than 5.0 s (Fig. 4f and Supplementary Movie 3).

Discussion

A conductive interface between insects and electronics was formed by attaching a self-adhesive, flexible film electrode to the insect's body using a biocompatible liquid. The adhesive strength depended on the thickness of the film and the type of liquid used. Thinner films evidenced better durability against friction, and strong adhesion was achieved with water or ethanol. This method was effective on both insect exoskeletons and glass (Supplementary Fig. 6), indicating its potential for application to other insects and inorganic surfaces like those of mechanical robots.

To exploit fully the insect's natural behavior, its locomotion ability must remain unimpeded. The softer the films attached to the insect's abdomen, the less they affect its movement[16]. This new pre-formed adhesive layer, allows for the more stable integration of softer film-based electronics than conventional methods, reducing the impact on the insect's mobility. Insects can retain flexible abdominal movements even with the body surface stimulation component integrated onto the abdomen. They can climb a vertical wall and self-righting from upside-down (Supplementary Fig. 7). The electrodes can also be easily removed by applying ethanol between the attachment surfaces. Even after repeated use, the insect's chitinous surface remains undamaged after the film is removed (Supplementary Fig. 8).

We successfully triggered postural changes in insects using external electrical stimulation on their body surface, allowing controlled left and right turns. Directional contraction of the abdomen by electrical stimulation has been observed in the moth similarly[54], suggesting that surface-based control could work for other insects. To achieve this, it is necessary to delicately adjust the device and stimulus parameters to the biological characteristics of each insect species. The responses to body surface stimulation depends on the applied voltage and can be controlled within a 3–6 V range. Conventional electrical stimulation requires 3–4 V. While this study used an external device for stimulation, a small wireless stimulator can be used with the addition of a voltage booster circuit. In addition, although maintaining the integrity of the insect's surface is infeasible, polishing the insect's body surface before integrating the body surface stimulation film has been shown to reduce impedance (Supplementary Fig. 9). This suggests the potential to reduce the voltage required to control the insect by further reducing the interfacial impedance between abdominal surface and the film electrodes. The turning angle induced by the voltage condition has a large variation. This is due to individual differences and subtle differences in the attachment position. Further investigation of attachment methods to suppress this variation is still an issue. The surface stimulation setup includes the interface film and the stimulation film, with the adhesive interface facing up. This structure allows thin-film solar cells[16] or sensors to be easily attached to the insect's body by applying them from above. Using the same adhesive layer, films can be layered onto the insect's body, improving the functionality and adaptability of the integrated devices.

In conclusion, a stimulation component was developed that can be attached to an insect's abdomen surface, allowing control of cyborg insect movement without compromising major sensory organs. The

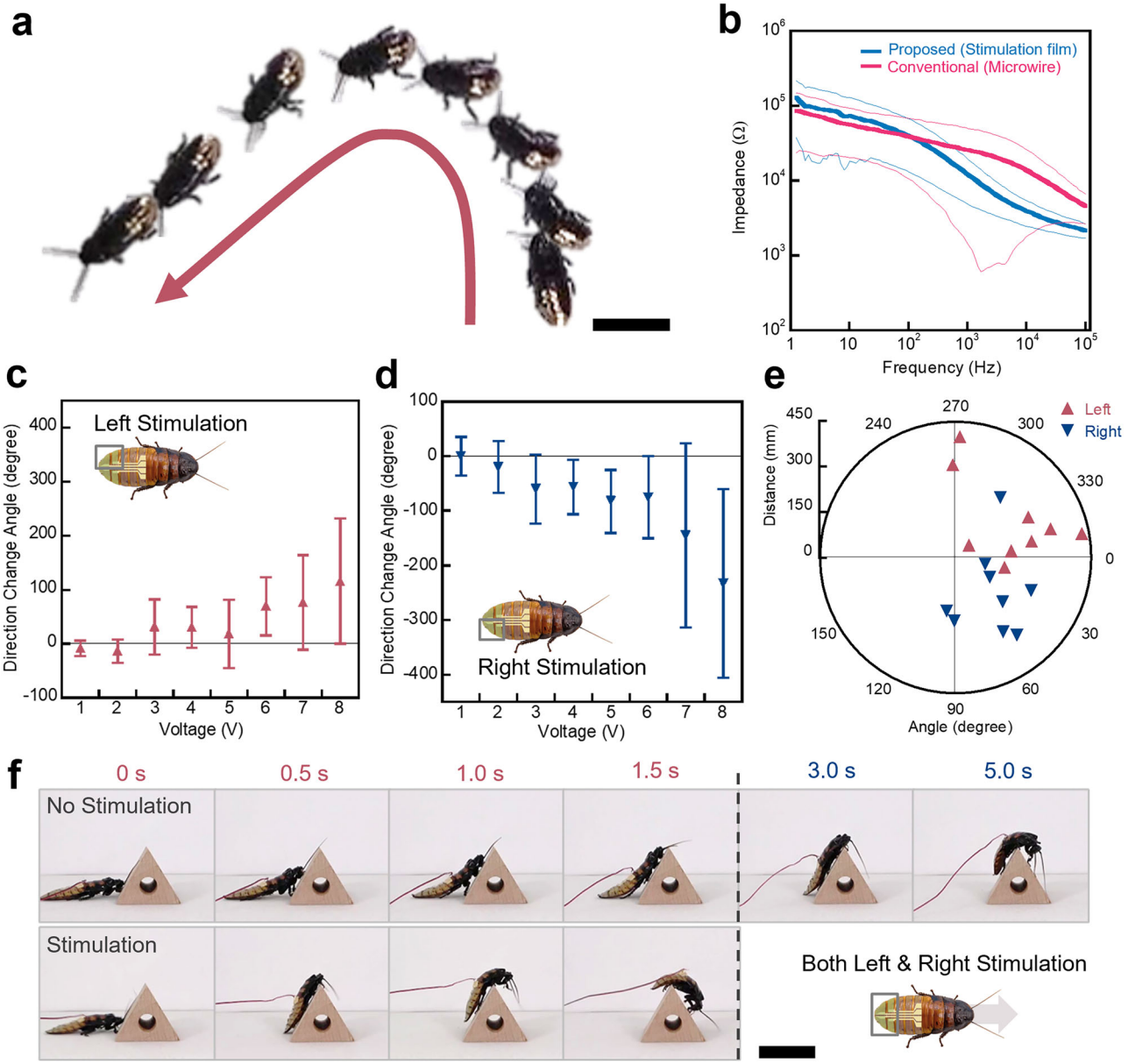

Fig. 4 | Verification of body surface stimulation components. a Multiple exposures and corresponding locomotion trajectories. By stimulating the left abdominal area, the subject turns to the left. Scale bar, 5 cm. **b** Insect-electrode impedance characteristics of the conventional implanted electrode and one adhered to the abdominal surface. Measurements were performed three times in three individuals each. The thin lines shows the standard deviation for each data point. **c, d** Change in turning angle depending on the voltage (42 Hz, Duty ratio 50%—single bipolar square-wave pulse, 1 ~ 8 V, 2 sec) when stimulating the left (**c**) and right (**d**) abdominal areas. In each condition, tests were performed three times in three individuals each. The upper and lower lines show the standard deviation. **e** Polar graph of position transition at 6 V stimulation from pre-stimulus to post-stimulus. **f** Effects on time taken to traverse an obstacle without stimulation and when stimulated to move straight. Scale bar, 4 cm. All photographs are brightness adjusted.

biocompatible adhesion method and the pre-formed adhesive structure formed by abdominal movements reduce damage to the insect during and after integration. Since the insect's major sensory organs are unaffected, it retains its natural behavior. This helps it navigate obstacles through normal sensory perception and allows more predictable behavior when not being controlled. By continuing to replace the artificial components with flexible, lightweight materials, cyborg insects can eventually surpass the abilities of natural organisms.

Methods

Experimental animals and rearing environment

This study used *G. portentosa* due to its high robustness and good mobility. A distinguishing feature between male and female *G. portentosa* is the presence or absence of thoracic exoskeletal protrusions. However, no distinction between males and females was made in this experiment. Only individuals with a body length of 4.5 cm or more, classifying them as adults, were used. The insects were kept in a rearing case measuring 26 cm in width, 14 cm in depth, and 20 cm in height, with husk chips as bedding. The rearing temperature was maintained between 25 and 38 °C. Insect jelly was provided regularly, ensuring that the supply never ran out. Experiments using insects were conducted in a common environment, with a room temperature of around 24 °C and a humidity of 40–60%. The invertebrates including insects used in this study do not require ethics approval for animal experiments according to the National Advisory Committee for Laboratory Animal Research.

Fabrication of interfacial film

A glass substrate was treated with oxygen plasma at 300 W for 10 min (PC-300, Samco). PSS solution (PSS/Water = 30 mg/ml) was spin-coated onto the glass substrate (50 mm × 50 mm) at 1000 rpm for 30 s (MS-B100, Mikasa). The substrate was heated at 110 °C for 5 min to form a sacrificial layer. Next, a SEBS solution (Tuftec H1221, 7.5 wt% in toluene) was spin-coated at 2000 rpm for 1 min to form a film approximately 1 μm thick after heating at 110 °C for 10 min. A 125 μm thick polyimide film was processed into a 56 mm × 56 mm frame with a 44 mm × 44 mm hole using a laser cutter. The frame was adhered to the SEBS surface using a diluted SEBS solution, and then heated at 110 °C for 10 min to dry the SEBS solution and secure the frame. The sacrificial layer was dissolved by immersing the substrate in water for approximately 1 h, allowing the film and frame to be peeled off the substrate.

Fabrication of wiring film

The glass substrate was treated with oxygen plasma at 300 W for 10 min. Next, a fluorinated polymer layer (Novec 1700:7100 = 1:5) was spin-coated onto a 50 mm × 50 mm glass substrate at 1000 rpm for 1 min. Following this, a chemical vapor deposition (CVD) system (PDS2010, KISCO) was used to deposit a 2 μm thick parylene layer. After treating the substrate with oxygen plasma at 300 W for 1 min, Cr (3.5 nm, 0.2 Å/s) and Au (100 nm, 1.5 Å/s) were deposited.

Fabrication of self-adhesive body surface stimulation film

The glass substrate was treated with oxygen plasma at 300 W for 10 min. Then, a PSS solution was spin-coated onto a 24 mm × 24 mm glass substrate at 1500 rpm for 30 s. The substrate was heated at 110 °C for 5 min to form a sacrificial layer. Next, a SEBS solution (7.5 wt% in toluene) was spin-coated at 2000 rpm for 1 min and heated at 110 °C for 10 min to form a film approximately 1 μm thick. The substrate was then treated with oxygen plasma at 50 W for 7 s, and Au (50 nm, 0.3 Å/s) was deposited by thermal evaporation. A 125 μm thick polyimide film (UPILEX, UBE Corporation) was laser-cut (Ether Laser Pro, SMART DIYs) into a 28 mm × 28 mm frame with a 20 mm × 20 mm hole and attached to the SEBS/Au surface using a diluted SEBS solution. The substrate was heated at 110 °C for 10 min to dry the SEBS solution and bond the frame. After soaking in water for approximately 1 h to dissolve the sacrificial layer, the electrode was peeled off the substrate.

Tensile test

A jig was 3D printed (form3, Formlabs) using Resin (Black Resin, Formlabs). The printed jig was cut into 5 mm squares using a CO2 laser cutter (SMART DIYs, Etcher Laser Pro). Insect abdomen exoskeleton pieces were fixed to the jig with double-sided tape (Nystack 5 mm wide, NICHIBAN). A 125 μm thick polyimide film was laser-cut into a 24 mm × 24 mm frame with a 9 mm × 9 mm hole using a laser cutter, and the frame was attached to each film. The film frame was fixed to the lower jig with double-sided tape. The upper jig with the insect exoskeleton pieces and the lower jig with the film frame were aligned on a tensile testing machine (EZ-LX, SHIMADZU). Adhesion was achieved by applying and volatilizing a liquid. Commercial electrode paste (ElefixV ZV-401E, Nihon Kohden) were used. For measurement, the 0.5 μm thick parylene/Au film was attached to the frame in the same manner as the wiring film, and the exoskeleton and parylene/Au were attached using an approximately 1 mm thick electrode paste. The tensile test was performed at a common speed of 1 mm/min.

Tensile tests with varying film thicknesses and drying times were conducted using Au/SEBS films with thicknesses of 1 μm, 5 μm, and 10 μm. The films were fabricated similarly to the self-adhesive body surface stimulation film. For the 5 μm and 10 μm films, the SEBS solution concentrations and spin-coating conditions were as follows: 5 μm films used a 15 wt% SEBS solution at 1000 rpm, and 10 μm films used a 22.5 wt% SEBS solution at 1000 rpm. The liquid was anhydrous ethanol was used. The volatilization times were set to 0 min, 20 min, and 60 min. The adhesion energy was calculated as the integral of the tensile distance and load. The film of 50 nm gold deposited on 500 nm-thick parylene was used to check the adhesion to the exoskeleton in a similar method.

Tensile tests with different liquids were conducted using different liquids: polar solvents (ethanol and deionized water) and a non-polar fluorinated solvent (Novec7100). A control experiment was also performed without any liquid. Using a SEBS thickness of 10 μm for an Au/SEBS film. The volatilization time for all tests was set to 60 min. In each condition, the test was performed three times. Adhesion to glass was also evaluated in the same method.

Friction test

The friction tests employed a friction tester (FPR2200, RHESCA), applying a 50 g load from above at a speed of 20 mm/s. Impedance measurements of the samples were taken with an LCR meter (ZM2376, NF). Two types of electrodes were fabricated, both with a line width of 5 mm. For both types, connections to the LCR meter were made with parylene/Au films approximately 1 μm thick, which were attached to the glass substrate with double-sided tape at both ends. The first type involved attaching SEBS/Au films (1, 5, 10 μm thick) to the glass substrate using a wet-volatile process with ethanol, followed by attaching a 1 μm thick Parylene film on top. The second type utilized a wet electrode adjusted to approximately 1 mm thick on the glass substrate, with a 1 μm thick parylene layer and 50 nm Au deposited on top via thermal evaporation, ensuring that the Au was in contact with the commercial electrode. In each condition, the test was performed once.

Evaluation of Au/SEBS ethanol permeability

A small bottle was filled with 5 g of ethanol and covered with a 50 nm gold film deposited on top of a 1,10 μm thick film of SEBS. As a reference, a sample without a cover was prepared. The samples were placed in a desiccator at room temperature.

Evaluation of the wet-volatile process stability

To evaluate the wet-volatile process stability, a 1 μm thick layer was attached to cover the dorsal surface of the insect's abdomen. The adhesive non-adhesive interleaving structure was formed by inducing abdominal movement multiple times. A parylene/Au film (3 mm × 30 mm) was attached on top of this structure for the parylene layer to contact the SEBS, spanning four abdominal segments (2–7). After inducing self-righting behavior three times, impedance measurements were taken at both ends of the parylene/Au film. For comparison, measurements of the parylene/Au conductivity were also performed using a resin-based skin adhesive (Spirit Gum, Mitsuyoshi). An impedance value above 1 kΩ was considered indicative of failure, while values below 1 kΩ were considered to indicate retained conductivity. Three thicknesses of parylene (0.5, 1.0, 2.0 μm) were tested, with each thickness being evaluated three times across three individuals. In each condition, tests were performed three times in three individuals each.

Measurement of impedance between the exoskeleton and electrode

The impedance between the stimulation components adhered to the insect and the sixth and seventh-eighth abdominal segments was measured. Measurements were conducted over a frequency range of 1 Hz to 100 kHz. The impedance change with time at 1 kHz was also recorded. Testing was performed three times across three specimens. For comparison, similar measurements were taken using conventional electrode wires inserted into the insect's body. Electrode wires were inserted into the 5th abdominal segment and the cerci, and impedance measurements were conducted. Measurements were performed three times in three individuals each.

Evaluation of response to electrical stimulation

The stimulation components were configured on the exoskeleton, and the subject's turning angle and movement position before and after stimulation were recorded under various voltage conditions. Stimulation was applied at voltages ranging from 1 to 8 V in 1 V increments, using a 42 Hz, 50% duty

cycle single bipolar square-wave pulse for 2 s. The procedure was recorded with a camera positioned above the subject, and its movements were analyzed. Each voltage condition was tested three times across three individuals for both the left and right sides. In each condition, tests were performed three times in three individuals each.

Data Availability

Data is provided within the manuscript or supplementary information files.

Received: 6 October 2024; Accepted: 13 February 2025;
Published online: 13 March 2025

References

1. Romano, D. et al. A review on animal-robot interaction: from bio-hybrid organisms to mixed societies. *Biological Cybernetics* **113**, 201–225 (2019).
2. Takemori, T. et al. Gait design of a snake robot by connecting simple shapes. *SSRR 2016 - International Symposium on Safety, Security and Rescue Robotics*, 189–194 (2016).
3. Bing, Z. et al. Lateral flexion of a compliant spine improves motor performance in a bioinspired mouse robot. *Sci. Robot.* **8**, 85 (2023).
4. Xie, Z. et al. Octopus-inspired sensorized soft arm for environmental interaction. *Sci. Robot.* **8**, 84 (2023).
5. Yun, S. et al. Remote-controlled fully implantable neural stimulator for freely moving small animal. *Electronics* **8**, 6 (2019).
6. Zhou, Z. et al. Pigeon robot for navigation guided by remote control: system construction and functional verification. *J Bionic Eng.* **18**, 184–196 (2021).
7. Kim, D. et al. Parasitic robot system for waypoint navigation of turtle. *J Bionic Eng.* **14**, 327–335 (2017).
8. Kobayashi, N. et al. Artificial control of swimming in goldfish by brain stimulation: Confirmation of the midbrain nuclei as the swimming center. *Neurosci. Lett.* **452**, 42–46 (2009).
9. Xu, N. et al. Developing biohybrid robotic jellyfish (*Aurelia aurita*) for free-swimming tests in the laboratory and in the field. *Bio. Protoc.* **11**, e3974 (2021).
10. Vo-Doan, T. et al. A cyborg insect reveals a function of a muscle in free flight. *Cyborg Bionic Syst.* **2022**, 9780504 (2022).
11. Bozkurt, A. et al. MEMS based bioelectronic neuromuscular interfaces for insect cyborg flight control. *2008 IEEE 21st International Conference on Micro Electro Mechanical Systems*. 160–163 (2008).
12. Yu, L. et al. Experimental verification on steering flight of honeybee by electrical stimulation. *Cyborg Bionic Syst.* **2022**, 9895837 (2022).
13. Tran-Ngoc, P. et al. Intelligent insect-computer hybrid robot: installing innate obstacle negotiation and onboard human detection onto cyborg insect. *Adv. Intell. Syst.* **5**, 2200319 (2023).
14. Liu, P. et al. Omnidirectional jump control of a locust-computer hybrid robot. *Soft Robotics* **10**, 40–51 (2023).
15. Nguyen, H. et al. Efficient autonomous navigation for terrestrial insect-machine hybrid systems. *Sens. Actuators B Chem.* **376**, 132988 (2023).
16. Kakei, Y. et al. Integration of body-mounted ultrasoft organic solar cell on cyborg insects with intact mobility. *npj Flex. Electron.* **6**, 78 (2022).
17. Hayashi, T. et al. Cyborg Insects Powered by An Insect-Mountable Biofuel Cell. *2022 International Symposium on Micro-NanoMechatronics and Human Science, MHS 2022*., 1–3 (2022).
18. Reissman, T. et al. Electrical power generation from insect flight. *Active and Passive Smart Structures and Integrated Systems 2011*, 797702 (2011).
19. Dirafzoon, A. et al. Poster abstract: Cyborg-insect networks for mapping of unknown environments. *2014 ACM/IEEE International Conference on Cyber-Physical Systems*, 216–216 (2014).
20. Iyer, V. et al. Living IoT: A Flying Wireless Platform on Live Insects. *MobiCom '19: 25th Annual International Conference Mobile Computing Networking* **5**, 1–15 (2019).
21. Lin, Q. et al. Resilient conductive membrane synthesized by in-situ polymerisation for wearable non-invasive electronics on moving appendages of cyborg insect. *npj Flex. Electron.* **7**, 42 (2023).
22. Proctor, J. L. & Holmes, P. The effects of feedback on stability and maneuverability of a phase-reduced model for cockroach locomotion. *Biol. Cybern.* **112**, 387–401 (2018).
23. Weihmann, T. et al. Speed dependent phase shifts and gait changes in cockroaches running on substrates of different slipperiness. *Fron. Zool.* **14**, 54 (2017).
24. Domenici, P. et al. Cockroaches keep predators guessing by using preferred escape trajectories. *Curr. Biol.* **18**, 1792–1796 (2008).
25. Tsukuda, Y. et al. Calmbots: Exploring Madagascar Cockroaches as Living Ubiquitous Interfaces. *Universal Access in Human-Computer Interaction*. *Novel Design Approaches Technologies.* **13308**, 522–541 (2022).
26. Latif, T. & Bozkurt, A. Line following terrestrial insect biobots. *2012 Annual International Conference of the IEEE Engineering in Medicine and Biology Society*, 972–975 (2012).
27. Comer, C. & Baba, Y. Active touch in orthopteroid insects: Behaviours, multisensory substrates and evolution. *Philos. Trans. R Soc. Lond. B Biol Sci.* **366**, 3006–3015 (2011).
28. Ye, S. et al. The antennal system and cockroach evasive behavior. I. Roles for visual and mechanosensory cues in the response. *J. Comp. Physiol. A Neuroethol. Sens. Neural Behav. Physiol.* **189**, 89–96 (2003).
29. Camhi, J. M. & Tom, W. The escape behavior of the cockroach *Periplaneta americana*. *J. Comp. Physiol.* **128**, 193–201 (1978).
30. Li, G. & Zhang, D. Brain-computer interface controlled cyborg: Establishing a functional information transfer pathway from human brain to cockroach brain. *PLoS ONE* **11**, e0150667 (2016).
31. Erickson, J. C. et al. Effective stimulus parameters for directed locomotion in Madagascar hissing cockroach biobot. *PLoS ONE* **10**, e0134348 (2015).
32. Li, Y. *et al*. Cercus electric stimulation enables cockroach with trajectory control and spatial cognition training. *Cyborg Bionic Syst*., 0154 (2024).
33. Liu, Z. et al. Locomotion control of cyborg insects by charge-balanced biphasic electrical stimulation. *Cyborg Bionic Syst.* **5**, 0134 (2024).
34. Sanchez, C. J. et al. Locomotion control of hybrid cockroach robots. *J R Soc Interface.* **12**, 20141363 (2015).
35. Camhi, J. M. Behavioral switching in cockroaches: transformations of tactile reflexes during righting behavior. *J. Comp. Physiol.* **113**, 283–301 (1977).
36. Visvanathan, K. & Gianchandani, Y. B. Locomotion response of airborne, ambulatory and aquatic insects to thermal stimulation using piezoceramic microheaters. *J. Micromech. Microeng.* **21**, 125002 (2011).
37. Lin, Q. et al. H. A newly developed chemical locomotory booster for cyborg insect to sustain its activity and to enhance covering performance. *Sensors Actuators B: Chemical* **399**, 134774 (2024).
38. Dong, K. et al. Scalable electrophysiology of millimeter-scale animals with electrode devices. *BME Front.* **4**, 0034 (2023).
39. Shoji, K. et al. Autonomous environmental monitoring by self-powered biohybrid robot. *2016 IEEE International Conference on Mechatronics and Automation*, 629–634 (2016).
40. Chiu, C. W. et al. Electrode-immune system interface monitor through neural stimulation in American cockroach (*Periplaneta Americana*). *Electrochimica Acta* **68**, 81–87 (2012).
41. Zhou, Z. et al. Progresses of animal robots: a historical review and perspectiveness. *Heliyon* **8**, e11499 (2022).
42. Sato, H. & Maharbiz, M. M. Recent developments in the remote radio control of insect flight. *Front Neurosci.* **4**, 199 (2010).
43. Latif, T. et al. In vitro electrochemical assessment of electrodes for neurostimulation in roach biobots. *PLoS ONE* **13**, e0203880 (2018).
44. Bozkurt, A. et al. Insect-machine interface based neurocybernetics. *IEEE Trans. Biomed. Eng.* **56**, 1727–1733 (2009).

45. Camhi, J. M. & Johnson, E. N. High-frequency steering maneuvers mediated by tactile cues: antennal wall-following in the cockroach. *J Exp Biol.* **202**, 631–643 (1999).
46. Baba, Y. et al. Collision avoidance by running insects: Antennal guidance in cockroaches. *J Exp Biol.* **213**, 2294–2302 (2010).
47. Harley, C. M. et al. Characterization of obstacle negotiation behaviors in the cockroach, *Blaberus discoidalis*. *J Exp Biol.* **212**, 1463–1467 (2009).
48. Fraser, P. J. Cercal ablation modifies tethered flight behaviour of cockroach. *Nature* **268**, 523–524 (1977).
49. Jiang, Y. et al. A universal interface for plug-and-play assembly of stretchable devices. *Nature* **614**, 456–462 (2023).
50. Vincent, J. F. V. & Wegst, U. G. K. Design and mechanical properties of insect cuticle. *Arthropod Struct Dev.* **33**, 187–199 (2004).
51. Li, C. et al. Cockroaches use diverse strategies to self-right on the ground. *J Exp Biol.* **222**, jeb186080 (2019).
52. Ritzmann, R. E. et al. Convergent evolution and locomotion through complex terrain by insects, vertebrates and robots. *Arthropod Structure Development* **33**, 361–379 (2004).
53. Yamagishi, K. et al. Tissue-adhesive wirelessly powered optoelectronic device for metronomic photodynamic cancer therapy. *Nat Biomed Eng.* **3**, 27–36 (2019).
54. Tsang, W. M. et al. Flexible split-ring electrode for insect flight biasing using multisite neural stimulation. *IEEE Trans Biomed Eng.* **57**, 1757–1764 (2010).

Acknowledgements

This work was partially supported by the Japan Society for the Promotion of Science under its Grants-in-Aid for Scientific Research (KAKENHI) (Nos. JP22K21343 and JP23K26077), Japan Science and Technology Agency (JST) under its JST-Mirai Program (No. JPMJMI21I1), and RIKEN Junior Research Associate Program.

Author contributions

S.K., H.S., S.U., K.F., and T.S. conceived of the main idea. S.K., S.L., and K.F. designed experiments. S.K. and K.A conducted experiments. S.K. analyzed the data. Z.J. and X.C. provided the self-adhesive body surface stimulation film fabrication technology. T.Y. prepared the environment for the fabrication test. All the authors discussed the results and commented on the manuscript. S.K. and K.F. wrote the manuscript. S.U., K.F., and T.S. supervised the project.

Competing interests

The authors declare no competing interests.

Additional information

Supplementary information The online version contains supplementary material available at https://doi.org/10.1038/s41528-025-00387-7.

Correspondence and requests for materials should be addressed to Shinjiro Umezu, Kenjiro Fukuda or Takao Someya.